

New Interpretation of the Valence Tautomerism of 1,6-Methano[10]annulenes and Its Application to Fullerene Derivatives

Cheol Ho Choi and Miklos Kertesz*

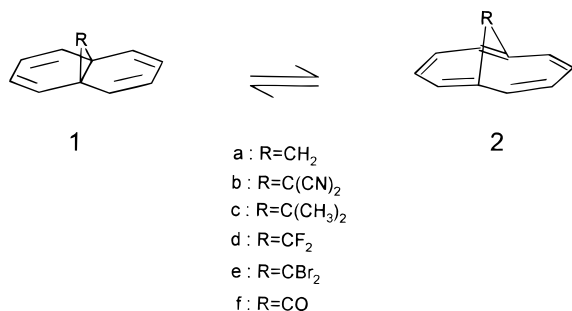
Department of Chemistry, Georgetown University, Washington, DC 20057-1227

Received: January 14, 1998; In Final Form: February 25, 1998

Relaxed potential energy surface scans of 1,6-methano[10]annulene and its derivatives have been calculated using Hartree–Fock (HF), density functional (DFT), and second-order Møller–Plesset perturbation theory (MP2) in the pursuit of nonclassical structures corresponding to an extremely long C₁–C₆ bond (~1.8 Å). Substituents affect the relative stabilities between the aromatic and the bisnorcaradiene forms, but their effects on the minima positions are moderate. We attribute the absence of a static C–C bond length in the vicinity of 1.8 Å to the well-defined inherent minima of cyclopropane in its singlet state (~1.5 Å) and trimethylene in its triplet state (~2.6 Å), which serve as the basis of our fragment analysis. The 1,6 bonding in these molecules is associated with a shallow potential well, in agreement with the Woodward–Hoffmann rules rather than to the existence of a static intermediate structure with a very long C–C bond. These results are in qualitative agreement with recent temperature-dependent ¹³C NMR experiments of Dorn et al. The trends in the C₁–C₆ bridgehead bonding are well-reproduced by the correlated calculations and to a lesser extent even by the HF calculations. However, simple electron donation/withdrawal arguments fail for this series. Due to the similarity in the delocalization energy of 1,6-methano[10]annulenes and disubstituted methano–buckyballs, predictions are made concerning the structural preferences for some disubstituted methano–fullerenes and –fulleroids. In contrast to general expectations open [6,6] methanofullerenes may exist. Major differences between methano[10]annulenes and methanofullerenes are derived from the constraints concerning the bookfolding angle that are strong in the latter and moderate in the former.

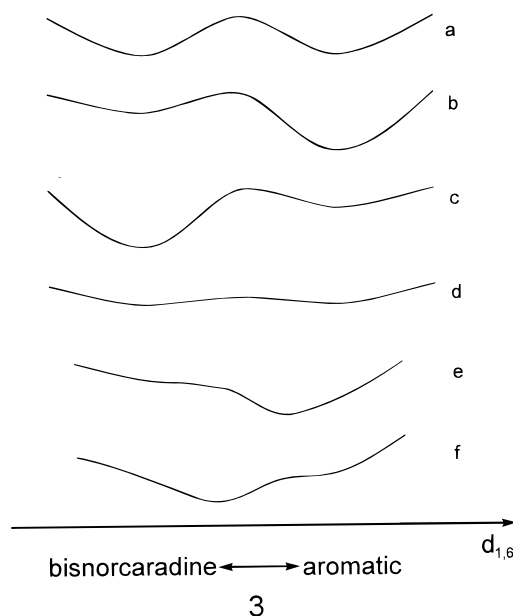
Introduction

For over 3 decades, the valence tautomerism (bisnorcaradiene form, **1**, and aromatic form, **2**) of 1,6-methano[10]annulene, **1a/2a**, and its derivatives,¹ **1b–d/2b–d**, has attracted considerable attention. Possible potential energy surfaces are schematically

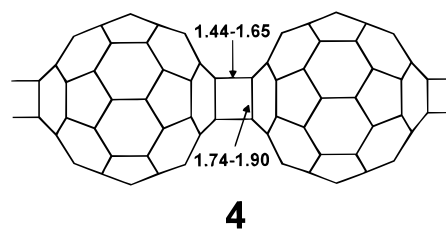


shown in **3** along the distance between the two bridgehead atoms 1 and 6, $d_{1,6}$. These represent either an interconverting mixture of a bisnorcaradiene form and an aromatic form, as shown in **3a–c**, separated by a small energy barrier. Alternatively, they may have a minimum corresponding to a “nonclassical” intermediate structure, **3d–f** with very unusual bond distances around 1.8 Å such as that found in the 11,11-dimethyl derivative.²

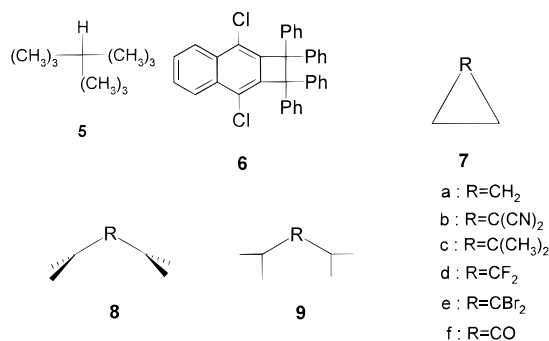
Recently, powder X-ray analysis of polymeric buckyballs, **4**, has indicated the possibility of C–C bond distances that are also in this very unusual range of 1.74–1.90 Å³, although the



large standard deviations make these data compatible with an interpretation involving stretched single C–C bonds of around



1.6 Å on the basis of large-scale density functional geometry optimizations.⁴ The $d_{1,6}$ bonds mentioned above for the **1/2** tautomerization are even longer than the most stretched C–C single bonds, such as those found in **5** (1.62 Å)⁵ and **6** (1.72



Å).⁶ These very large bond lengths found in **5** and **6** are consistent with bond distances obtained by geometry optimization using nonlocal density functional theory (DFT) that includes electron correlation effects originating in bond stretching.⁷

Not only do some members of the 1,6-methano[10]annulene series have unusual bond distances but they also exhibit a very strong dependency on bridge substitutions at C₁₁,² showing a large spread of $d_{1,6}$ values varying between 1.54 and 2.27 Å. Burgi et al.⁸ have pointed out that this pericyclic ring opening is an allowed concerted process in the Woodward–Hoffmann sense. The wide variations in bridgehead distances have been rationalized by Simonetta et al.^{2e} using the analogy of cyclopropane, **7**, where the introduction of π -donating at position 1 lengthens all CC bonds in the ring, while π -acceptors strengthen the C₂–C₃ bond and weaken the other two.⁹ Since the C₂–C₃ bond distance variations are much smaller than those of $d_{1,6}$, this interpretation appears to be incomplete and, as will be discussed below, fails to explain the rather similar behavior of the parent compound and the difluoro derivative, or the large difference between the dibromo and difluoro derivatives. The temperature dependency of $d_{1,6}$ of some derivatives further complicates the understanding of this bonding and has yielded the concept of “fluxional” bonding.^{1b} Recently, Kaupp and Boy¹⁰ have concluded that “the reported temperature factors are not normal and that an unrecognized structural disorder [in the crystal structures] gave rise to averaged values [of $d_{1,6}$] from coexisting fractions of **1** and **2**”.

The observed range of ¹³C NMR chemical shifts of atoms 1 and 6 of various 11,11-disubstituted 1,6-methano[10]annulenes also exhibits a substituent effect at C₁₁.^{1c,11,12} In some of these molecules, the temperature dependency of the chemical shift of atoms 1 and 6 has been observed and interpreted as a fast tautomerism¹² between the two forms, contrasting the results of X-ray experiments. Early potential surface calculations along the $d_{1,6}$ based on Hartree–Fock theory (HF/3-21G)^{2e} also supported this picture. However, recently, Dorn et al.¹³ have performed ¹³C CPMAS NMR experiments on the dimethyl derivative at low temperatures (10–100 K) and interpreted the results as a nonclassical structure having an unusual bond length, 1.8 Å corresponding to a potential energy surface such as **3e**, not as a fast tautomerization between two structures as would be the case for **3a**. On the basis of their NMR analysis and the earlier X-ray evidence, Dorn et al. also noted that this structure exhibits a strong temperature dependence. They offered two alternatives as possible sources of this temperature dependence: (1) the higher vibrational levels becoming more populated as temperature is increased and (2) temperature-

dependent intermolecular interactions. In this paper we show that alternative 1 of Dorn et al. fits nicely into the picture resulting from the DFT calculations for this member of the series, while substituent effects are also explained. Furthermore, Klingensmith et al.¹⁴ have used magnetic circular dichroism (MCD) spectroscopy to determine the molecular orbital ordering and have shown the presence of a strong transannular interaction between the two bridgehead atoms. However, whether this interaction can be considered as a bond is yet unclear.^{1d,2,15}

Recently, Mealli et al.¹⁶ have explained the effects of substituents on the transannular bond length by referring to electron donor–acceptor interactions and steric hindrance effects between the substituent and the naphthalene moieties on the basis of extended Hückel theory (EHT). Their interpretation is in contrast with their own ab initio Hartree–Fock (HF) results, especially regarding the value of the $d_{1,6}$ bond distance of the dimethyl derivative (1.8 Å). On the basis of this fact, Mealli et al. concluded that HF is not sufficient for interpreting this bonding, where the effects of delocalization, extreme bond stretching, and steric hindrances lead to a delicate balance resulting in the large variations observed for $d_{1,6}$.

In this paper, we attempt to qualitatively better understand the potential energy surface along $d_{1,6}$ on the basis of large-scale ab initio and density functional calculations that go beyond HF and to obtain an interpretation consistent with the experiments. To begin with, we shall present our results and observations of the potential surfaces of **1a–d/2a–d** along $d_{1,6}$. After that, we focus on 1,6-methano[10]annulene, **1a/2a**, by using a hypothetical fragmentation scheme which is comprised of the triplet excited state of cyclopropane stabilized by the delocalization of 10 π -electrons. This fragmentation allows the interpretation of substituent effects on $d_{1,6}$ that cannot be explained by electronegativity or steric arguments alone. On the basis of our results found in 1,6-methano[10]annulene and its derivatives, structural preferences in [5,6] and [6,6] ring junction adducts of C₆₀ (fulleroids and methanofullerenes, respectively) are also discussed. In agreement with expectations for all studied [5,6] substituted fullerenes (fulleroids), an open structure is found in the full geometry optimizations. However, while for some substituted [6,6] fullerenes (methanofullerenes) a closed structure is found in the geometry optimizations, exceptions are also found.

Computational Details

HF (Hartree–Fock), MP2 (second-order Møller–Plesset perturbation theory), and DFT (density functional theory) calculations have been performed by the Gaussian 94¹⁷ program using 3-21G, 6-31G*, and 6-311+G* basis sets. Lee, Yang, and Parr’s (LYP)¹⁸ correlation functional in combination with Becke’s three parameter hybrid (B3)¹⁹ exchange functional was used for the gradient-corrected density approximation. For all relaxed potential surface scans (full geometry optimization at each point), a regular 0.1 Å mesh of points was applied in the calculation. Nucleus-independent chemical shifts (NICS)²⁰ were computed with the GIAO (gauge-independent atomic orbital) method²¹ at the optimized B3LYP/6-31G* geometries. NICS provides a practical aromaticity index that can be calculated at the ring center (nonweighted mean of the heavy atom coordinates on the ring perimeter) with the Gaussian 94 program.²⁰

Potential Surfaces

Table 1 summarizes the locations of the minima of the fully optimized potential energy surfaces along the valence tautomerization coordinate $d_{1,6}$ for the bridged annulenes discussed in

TABLE 1: Calculated and Experimental $d_{1,6}$ (Å) of 1,6-Methano[10]annulene and Its Derivatives

	R		$d_{1,6}$
expt	C(CN) ₂	1b/2b	1.543 ^a
	C(CH ₃) ₂	1c/2c	1.770, ^b 1.826 ^b
	CH ₂	1a/2a	2.235 ^c
	CF ₂	1d/2d	2.269 ^d
HF/6-31G*	C(CN) ₂	1b/2b	1.511
	C(CH ₃) ₂	1c/2c	1.583
	CH ₂	1a/2a	1.576, 2.217
	CF ₂	1d/2d	1.623, 2.226
B3LYP/6-31G*	C(CN) ₂	1b/2b	1.559, 2.256
	C(CH ₃) ₂	1c/2c	2.168, ^e (1.7 ^f)
	CH ₂	1a/2a	2.285
	CF ₂	1d/2d	2.296
	CBr ₂	1e/2e	1.693, 2.243
	CO	1f/2f	2.377
MP2/6-31G*	C(CN) ₂	1b/2b	1.599, 2.237
	C(CH ₃) ₂	1c/2c	2.156
	CH ₂	1a/2a	2.251
	CF ₂	1d/2d	2.268

^a Taken from ref 2c. ^b Taken from ref 2d. ^c Taken from ref 2a.

^d Taken from ref 2b. ^e 2.170 as calculated with B3LYP/6-311+G*.

^f Approximate location of an inflection point.

this paper. They are arranged in the order of increasing experimental bridgehead distances. The HF trend follows this order, although the $d_{1,6}$ values tend to be too short, or the shorter minimum remains a minimum in disagreement with experiment. The corresponding correlated MP2 values tend to be too long, and for the dicyano case the longer minimum persists against experimental indications. The fact that electron correlation effects stabilize the delocalized (aromatic) structure over the localized (bisorcaradiene) structure has been pointed out before.²²

The B3LYP data are closer to MP2, but are between the MP2 and the HF values. The overall B3LYP trend is correct, although for the dicyano case it also predicts a double minimum; the longer one is not indicated by the experiment. The intermediate dimethyl case deserves detailed discussion: here the experimental values^{2a} (1.77–1.83 Å) are between the HF (1.58 Å) and the correlated minimum positions (2.16–2.17 Å).

We turn to the details of the potential surfaces in order to better understand this intermediate case. The relaxed potential energy surface scans as obtained with Hartree–Fock theory along $d_{1,6}$ are presented in Figure 1. The series of potential energy surfaces put the Hartree–Fock results in slightly more favorable light than the locations of the minima alone would. Starting from the dicyano end, where the HF minimum is correct, there is a shift toward the stabilization of the longer minimum relative to the shorter one in the following order: R = CMe₂, CH₂, CF₂. This ordering is qualitatively correct; the aromatic form is not sufficiently stabilized though, so even for the CF₂ case the shorter minimum remains present and is about 1 kcal/mol above the longer minimum, although according to the experiment the latter is likely the only minimum. However, this shortcoming of HF should not be surprising considering the fact that during the stretching of $d_{1,6}$ the electronic structure is being considerably reorganized and that the correlation energy changes are substantial, making HF inadequate for accurately describing this valence tautomerism. Stevenson and Zigler determined the relative stability of **1a** and **2a** as 5.7 kcal/mol²³ on the basis of a series of thermochemical reactions assuming the separate existence of two structures. In HF the two structures (**1a/2a**) exist as two almost equienergetic local minima. Mealli et al.¹⁶ explained some of the difficulties of the HF results by referring to the delicate balance of steric and

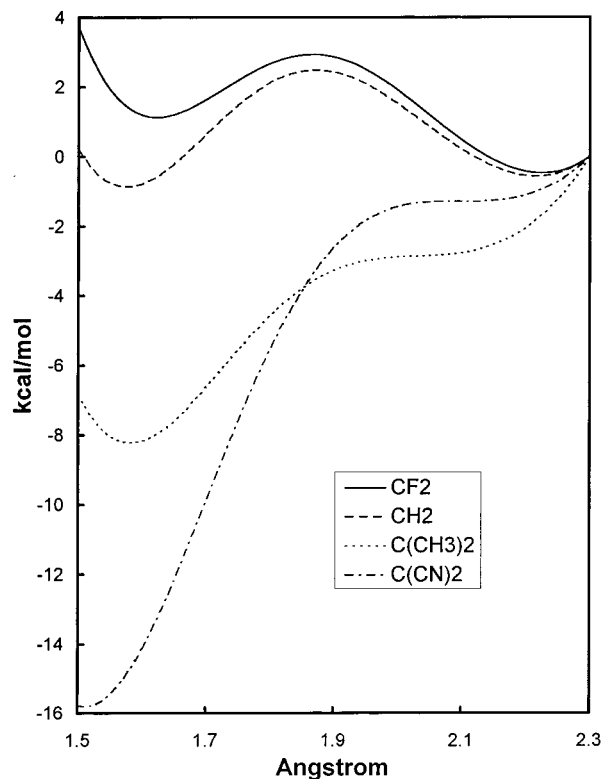


Figure 1. Potential energy surface scans along $d_{1,6}$ of 1,6-methano[10]annulene and its derivatives as calculated with HF/6-31G*.

electronic effects on the basis of their EHT analysis and questioned the adequacy of the uncorrelated HF calculations. We certainly agree with this assessment. However, it is worth pointing out that the order in which the substituents change the relative stabilities of the localized and delocalized forms is already correctly described at the HF level, indicating that the balance of electronegativity, delocalization, and steric effects is already quite well represented at this level of theory. It is the balance of localization/delocalization and simultaneous stretching of $d_{1,6}$ that needs the inclusion of electron correlation effects.

Figures 2 and 3 show the B3LYP density functional and the MP2 perturbation theoretic results, respectively. Some of these potential energy surfaces are very flat. However, these rather expensive calculations do not agree fully with the experiments either. Putting aside the CO and CBr₂ cases for the moment due to a lack of structural data, now the opposite behavior as compared to the HF method is observed, although the chemical trend is the same. In the sequence of substitutions, R = CF₂ and CH₂, the agreement with experiment is good; the CMe₂ case as a borderline case exhibits a very flat potential, but the C(CN)₂ case still exhibits both minima in contrast to the experimentally found single short minimum. It appears that while HF underestimates delocalization, these two correlated methods slightly overestimate it.²²

What is the “true” potential surface like? Even if one could perform a much higher level ab initio correlated total energy calculation with a very large basis set for these systems, the question of crystal packing energy would still remain. When the potential energy is flat, or the competing minima are within 1–3 kcal/mol of each other, crystal packing can easily tip the balance, making predictions of the location of the minima based on isolated molecule calculations invalid. Therefore, we conclude that the potential energy surfaces for the dicyano, dimethyl, and dibromo cases are likely to be very flat.

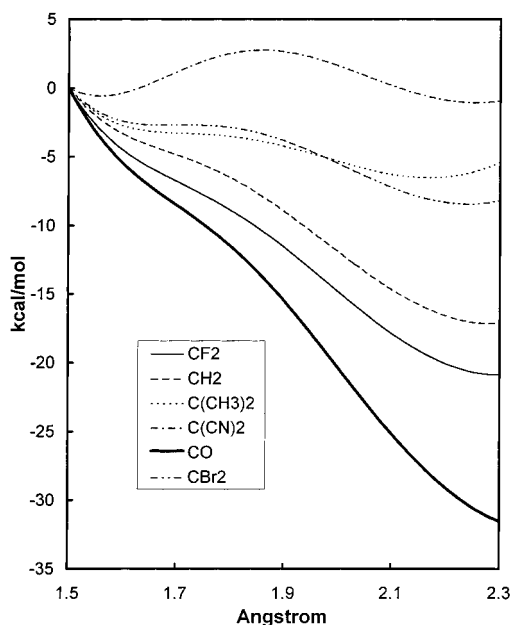


Figure 2. Potential energy surface scans along $d_{1,6}$ of 1,6-methano-[10]annulene and its derivatives as calculated with B3LYP/6-31G*.

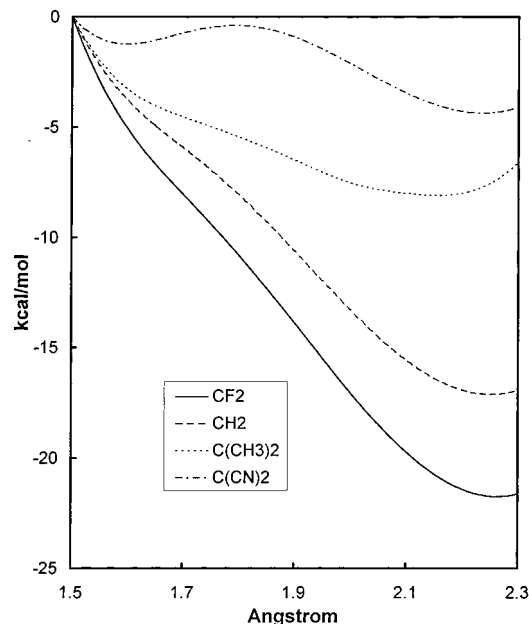


Figure 3. Potential energy surface scans along $d_{1,6}$ of 1,6-methano-[10]annulene and its derivatives as calculated with MP2/6-31G*.

Furthermore, for the dicyano case as suggested by the experiment the localized **1** form is more stable than the delocalized **2** form. The energy difference should be only a few kilocalories per mole.

The intermediate cases, with the dimethyl and dibromo substitution, are likely to exhibit a flat potential. This conclusion offers a natural explanation for the intermediate $d_{1,6}$ values obtained for the dimethyl case by X-ray diffraction. However, according to this interpretation these cases do not correspond to a static C–C bond length of about 1.8 Å but rather to an average resulting from a large amplitude mode along $d_{1,6}$. This conclusion is in qualitative agreement with the recent CPMA NMR study¹³ on **1c/2c** and also with Kaupp and Boy's comment.¹⁰ The temperature dependence of the $d_{1,6}$ bond for the dimethyl derivative results, therefore, from the flat and highly anharmonic nature of the potential, as suggested by

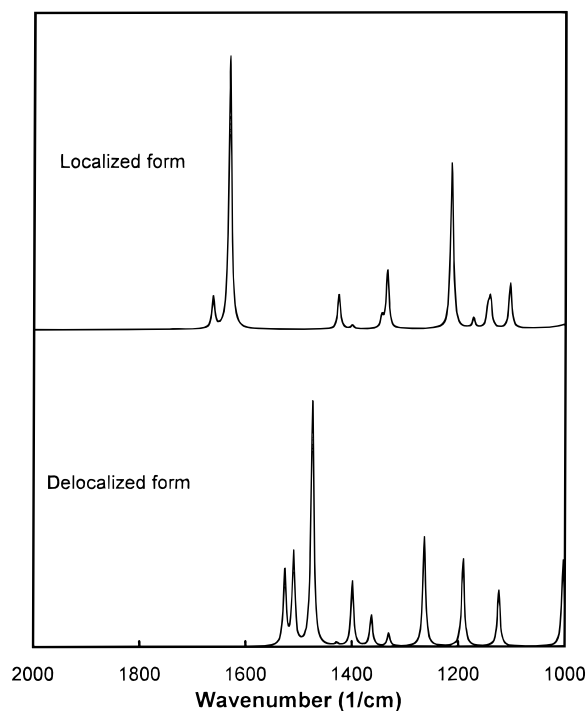


Figure 4. Predicted IR spectra of **1a** and **2a** as calculated with B3LYP/6-31G*.

alternative **1** in the paper by Dorn et al.¹³ mentioned in the Introduction.

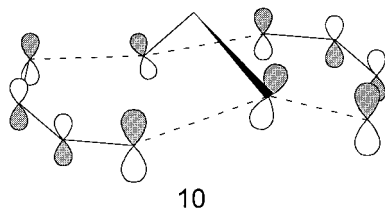
In order to study the substituent effects further, the potential energy surfaces of two further derivatives, **1e/2e** and **1f/2f**, were also evaluated with B3LYP/6-31G* and included in Figure 2 and Table 1. Because of the strong electron withdrawing carbonyl substituent in **1f/2f**, it is expected that the **1f** form should be preferred as found in the dicyano derivative. However, the result is the opposite and the **2f** form is preferred. In the case of the dibromo derivative, the potential energy surface is similar to that of the dimethyl derivative, although dibromo is expected to be the more strongly electron donating group and to behave similarly to the difluoro derivative. These observations indicate that the interpretation cannot be based on the simple electron withdrawing and donating arguments only.

The two tautomeric "structures" are sufficiently different to produce dramatically different vibrational spectra. An example of such a pair of calculated spectra of **1a/2a** is given in Figure 4. Unfortunately no vibrational spectra of any substituted 1,6-methano[10]annulene has been published in sufficient detail to allow a definite assignment. Such an assignment based on a predicted spectrum should provide further tests of the present theoretical results.

Trimethylene Fragmentation Model

A simple question arises. Why are the positions of the local minima at the bisnorcaradiene and aromatic forms not affected much by the substituents? In order to answer this question, a hypothetical scheme composed of a ring opening reaction (**7a** → **8a**) of a cyclopropane fragment followed by a 10π -electron delocalization step (**8a** → **2a**) is proposed, since this tautomerism can be viewed as an $8\pi + 2\sigma \rightarrow 10\pi$ -electron transformation, as illustrated in **10**.

Cyclopropane, **7**, and the trimethylene intermediate, **8** or **9**, have been thoroughly studied.²⁴ Because of its relative stability, most of the earlier studies have been devoted to the trimethylene structure **9** (dihedral angles are 0,0 using Hoffmann's definition



of the geometry^{24a}), where the terminal hydrogens are in the same plane as the carbon atoms. For our purposes, the more relevant conformation is the intermediate^{24a} **8**, where the π -orbitals of the terminal carbon atoms are in the plane of the carbon atoms. The frontier orbital diagrams of the parent cyclopropane ring opening reaction (**7a** \rightarrow **8a**) along C_2-C_3 as calculated with B3LYP/6-31G* is presented in Figure 5. Since, as the distance, C_2-C_3 increases, the bonding or antibonding character along C_2-C_3 is reduced, mostly two molecular orbitals, a_1 and b_2 , are perturbed, yielding a low-lying LUMO in the trimethylene,^{24a,16} **8a**.

For large bridgehead distances the molecule becomes a biradical and the triplet state becomes the true ground state as is manifested by the calculations for trimethylene, **8a** (see Figure 6). Although the energy of the triplet ground state as compared with that of the singlet ground state of **8a** is higher by 62.5 kcal/mol, it is very interesting that the triplet ground state has a minimum position around 2.6 Å along the C_2-C_3 reaction coordinate regardless of computational method used (see Table 2). (Due to geometric constraints present in **2** but not in **8**, $d_{1,6}$ in aromatic [10]annulenes is reduced from 2.6 to around 2.3 Å.) Furthermore, the minimum positions at 1.5 and 2.6 Å are not much affected by substituent effects either, as can be seen in Figures 7 and 8, while the relative stability between the singlet and triplet minima is clearly dependent on the substituents (see Figure 8). The C_2-C_3 bond length of the 1,1-dimethyl-substituted trimethylene is slightly shorter than for the other closest derivative due to the steric requirements of the rather bulky CH_3 group.

In Figure 8 where the relative molecular energy of the triplet state is shown, it is seen that the substituent effects reduce the triplet energy in the same order as that seen in Figures 2 and 3 for the annulenes (see the order of the $E_{rel} = E(\text{at triplet minimum}) - E(\text{at singlet minimum})$ values in Table 2 also), the dibromo derivative being the only exception. According to this result, a hypothesis is proposed, that is, *aside from steric effects the substituent, which stabilizes the triplet state of trimethylene more as compared to the singlet state of the corresponding cyclopropane derivative, will prefer the open structure (2) rather than the closed structure (1)*. Consequently, the strength preference for the localized (closed) structure in descending order should be $C(CN)_2 > C(CH_3)_2 > CH_2 > CF_2 \sim CBr_2 > CO$. Surprisingly, all three methods, including Hartree-Fock, predict the same sequence for all molecules considered, as can be seen from the last column of Table 2. This sequence is in agreement with the experimental data for the four members of the series for which experimental data are available. For the dibromo case, however, the B3LYP prediction based on the calculation of the whole molecule is that its tautomerization potential is more similar to the dimethyl case than to the difluoro case. On the other hand, the full B3LYP calculation for the CO case is in agreement with the above sequence. Steric effects explain the special dibromo case. It seems that electronegativity of the substituents does not correlate well with the structural preferences of this valence tautomerism.

In order to understand this exception, the bookfolding angles (Θ) of the naphthalene moiety, which may be a good measure

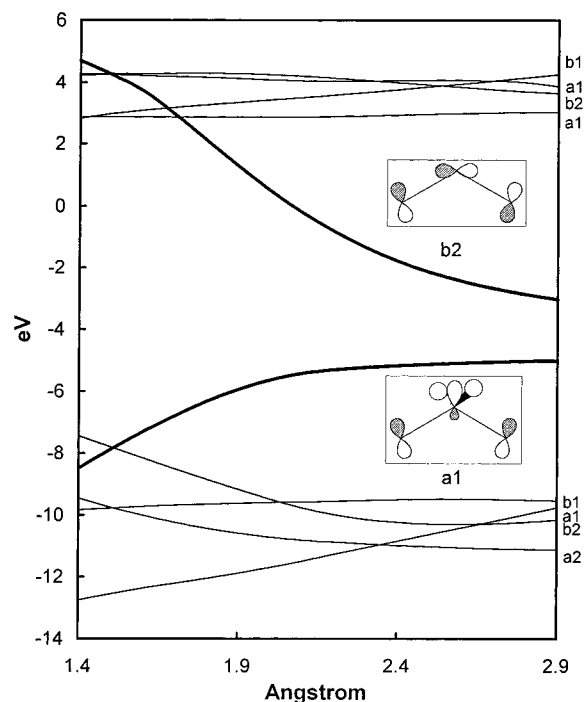


Figure 5. Orbital diagram along the C_2-C_3 bond of cyclopropane as calculated with B3LYP/6-31G*.

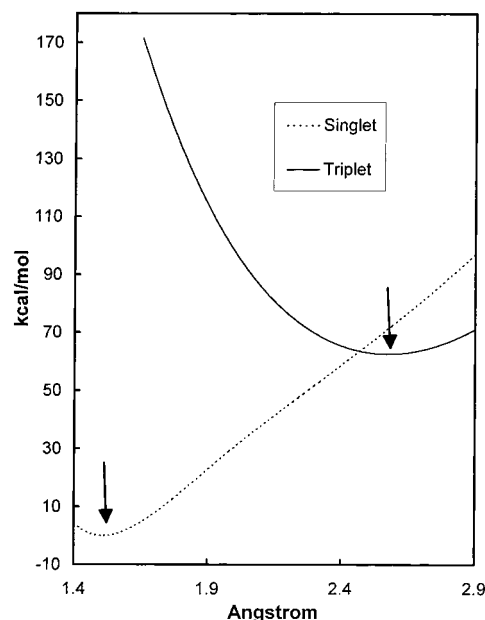


Figure 6. Total molecular energy of the singlet ground state (cyclopropane) and triplet excited state (trimethylene in the **8** conformation) along the C_2-C_3 bond as calculated with B3LYP/6-31G*. Arrows indicate the singlet and triplet minima where the $E_{rel} (=E(\text{at triplet minimum}) - E(\text{at singlet minimum}))$ was evaluated (see Table 2).

of steric hindrance between the substituents and the two rings, were compared. The calculated Θ value of **1b** is 148.7° which is in good agreement with experiment, 151.2° .² The Θ values of **2a-f** as calculated with B3LYP/6-31G* are 151.8 , 147.9 , 137.2 , 145.8 , 139.8 , and 155.4° , respectively. As expected, the relatively crowded **2c** and **2e** have small Θ values exhibiting large steric hindrance, while the least crowded **2f** shows the largest Θ among these derivatives. We conclude that in the dibromo derivative steric effects are large enough to reduce Θ sufficiently enough to destabilize the aromatic form. The experimental test of this prediction would be interesting.

TABLE 2: Calculated and Experimental C–C Bond Distances of Substituted Cyclopropanes (Singlet) and Trimethylenes (Triplet)

	R		cyclopropane (C_{2v})		trimethylene (C_{2v})		E_{rel}^a
			C ₁ –C ₂	C ₂ –C ₃	C ₁ –C ₂	C ₂ –C ₃	
HF/6-31G*	C(CN) ₂	1b/2b	1.520	1.478	1.524	2.568	47
	C(CH ₃) ₂	1c/2c	1.499	1.502	1.518	2.530	42
	CH ₂	1a/2a	1.497	1.497	1.510	2.567	38
	CF ₂	1d/2d	1.465	1.535	1.499	2.568	32
B3LYP/6-31G*	C(CN) ₂	1b/2b	1.540	1.487	1.527	2.582	73
	C(CH ₃) ₂	1c/2c	1.512	1.513	1.516	2.539	67
	CH ₂ ^b	1a/2a	1.509	1.509	1.507	2.576	63
	CF ₂	1d/2d	1.480	1.547	1.499	2.584	59
	CB _{r2}	1e/2e	1.494	1.525	1.481	2.586	59
	CO	1f/2f	1.474	1.572	1.497	2.606	54
MP2/6-31G*	C(CN) ₂	1b/2b	1.528	1.489	1.515	2.573	79
	C(CH ₃) ₂	1c/2c	1.504	1.510	1.509	2.525	73
	CH ₂	1a/2a	1.503	1.503	1.504	2.559	69
	CF ₂	1d/2d	1.473	1.545	1.495	2.575	64

^a Relative energies in kilocalories per mole of triplet ground state as compared to the singlet ground state $E_{rel} = E(\text{at triplet minimum}) - E(\text{at singlet minimum})$. ^b Shown in Figure 6.

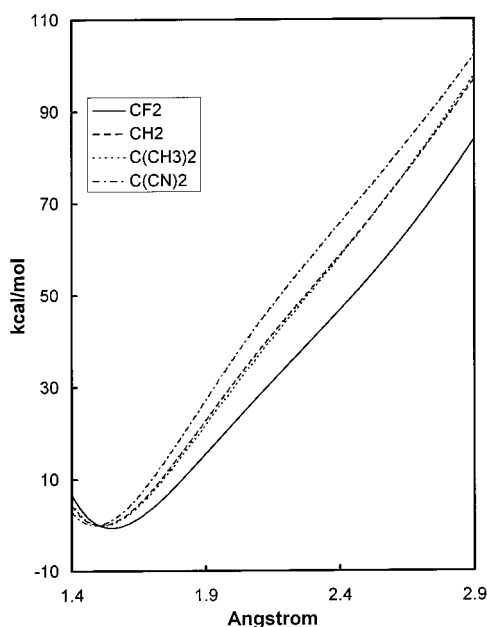


Figure 7. Total molecular energy of the singlet ground state of cyclopropane and its derivatives along the C₂–C₃ bond as calculated with B3LYP/6-31G*.

According to this interpretation, the CO derivative is delocalized primarily due to the smallest triplet–singlet energy difference (E_{rel} in Table 2) and not because it is the least crowded member of the series.

The aromatic stabilization energy of [10]annulene as compared with two butadienes and trimethylene in the **10** configuration is 4β within the simple Hückel theory. If we take the thermodynamic value for β ,²⁵ this stabilization energy amounts to about 60 kcal/mol. Although this is a very simple argument, it does indicate that the aromatic stabilization energy is significant. (This point is essential in the applications of this model to fullerenes, where the delocalization energy is large also.) The fact that the general trend of the substituent effects on the relative stabilization energy for **8** is the same as that for **2** indicates that the aromatic stabilization energies of **2** are rather insensitive to the substituents.

In order to further characterize the 10π -electron delocalization, NICS calculations were performed. Negative NICS values denote aromaticity (–11.5 for benzene) and positive NICS values antiaromaticity (28.8 for cyclobutadiene). Non-aromatics

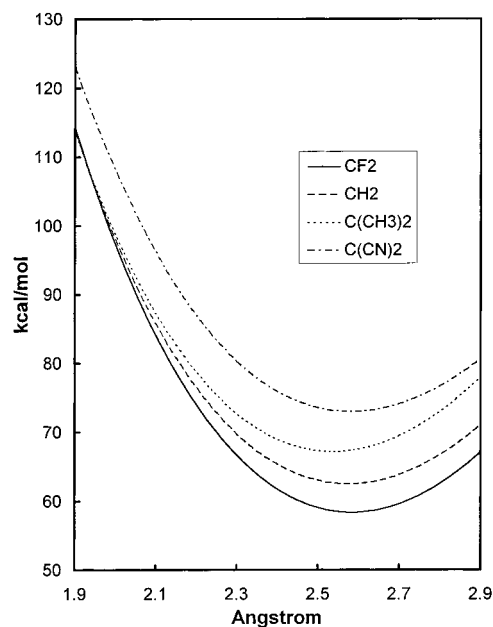


Figure 8. Total molecular energy of the triplet ground state of trimethylene and its derivatives along the C₂–C₃ bond as calculated with B3LYP/6-31G*. All energies are relative to their singlet ground states.

TABLE 3: Nuclear Independent Chemical Shift As Calculated with GIAO/B3LYP/6-31G*/B3LYP/6-31G* (ppm)

R		bisnorcaradine form, 1	aromatic form, 2
C(CN) ₂	1b/2b	–3.2	–15.2
C(CH ₃) ₂	1c/2c		–14.5
CH ₂	1a/2a		–15.2
CF ₂	1d/2d		–14.2

have NICS values close to zero (–2.1 cyclohexane). As another indicator of aromaticity, NICS correlates well with magnetic susceptibility exaltation and has the advantage of being less dependent on the ring size and can be used for individual rings in polycyclic systems.²⁰ The calculated NICS values are presented in Table 3. The NICS value of the aromatic form of the dicyano derivative decreases dramatically as compared to that of the bisnorcaradine form showing a substantial degree of aromaticity. Furthermore, the NICS value of the aromatic form is rather insensitive to the substituents, providing further support for the trimethylene fragmentation model.

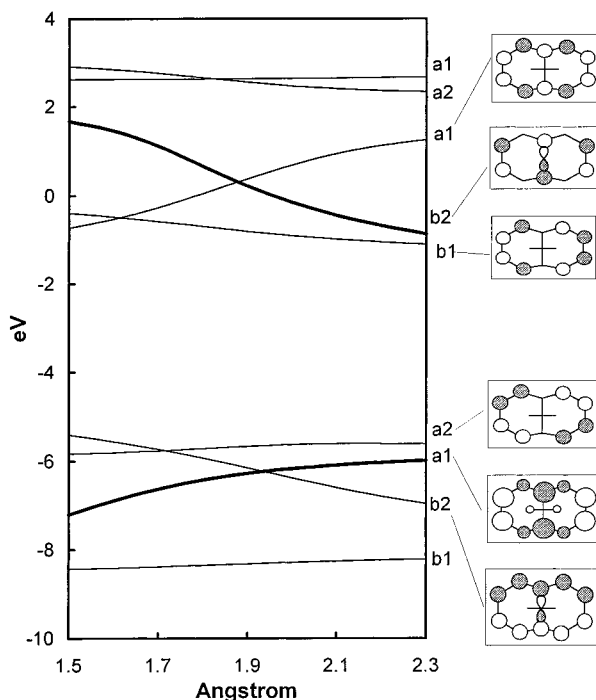


Figure 9. Orbital diagram along $d_{1,6}$ of 1,6-methano[10]annulene as calculated with B3LYP/6-31G*.

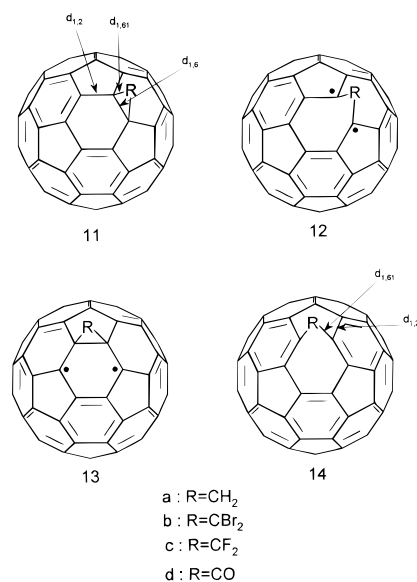
Orbital Interpretation

The Walsh diagram of 1,6-methano[10]annulene as calculated with B3LYP/6-31G* is presented in Figure 9. Since this is very similar to that of Mealli et al.¹⁶ obtained by EHT, we emphasize the connection to the trimethylene model.

Since the contribution of the $2p_z$ atomic orbitals from the trimethylene part is negligible, the HOMO (a_2) and LUMO (b_1) levels are virtually independent of $d_{1,6}$. The energy levels of the two b_2 orbitals are lowered by the reduced 1–6 antibonding interaction in the trimethylene part in the aromatic form. For the opposite reason, the two a_1 orbitals are raised. The thicker lines in Figure 9 correspond to the respective a_1 and b_2 frontier orbitals in Figure 5. However, the dispersion of the former—primarily due to normalization—is significantly reduced. In terms of Woodward–Hoffmann rules,^{26,27} this reaction is $[\pi(4s) + \sigma(2s) + \pi(4s)]$ disrotatory and has only one $\sigma(2s)$. Therefore it is thermally allowed and yields the filled a_1 orbital in Figure 9. In another orbital the two localized butadiene fragments are out of phase (only the in phase combination is shown in the diagram of 10). This orbital has no interaction with the middle two carbons, yielding the a_2 symmetry HOMO which is localized on the two butadiene fragments. This general observation dictates that there is only a small barrier between the two structures, **1** and **2**, which is consistent with the calculated potential surfaces with all substituents considered. For most substituents the balance tips in favor of one structure and there is in most cases only one well-defined minimum.

Applications to Fullerene Derivatives

There are interesting analogies to the **1/2** valence tautomerism in fullerene chemistry. The addition to the [6,6]-type bond ([6,6] refers to the bond at the fusion of a six-membered ring to another six-membered ring) in C_{60} results in a methanofullerene, **11** or **12**, while the addition to the [5,6]-fusion bond of C_{60} results in a fulleroid, **13** or **14**.²⁸ In both cases the tautomerism is between a $58\pi + 2\sigma$ system (closed structures **11** or **13**) as compared



with a 60π -electron system (open structures **12** or **14**). The tautomerism between **11** and **12** is analogous to the tautomerism of 1,6-methano[10]annulene, **1/2** discussed in this paper. On the basis of this analogy one would expect a systematic dependence of the length of the [6,6] connecting bond (denoted by $d_{1,6}$ in order to maintain the analogy) on the substituents.

Two, somewhat independent issues arise in the case of fullerene adducts: (i) the relative stability of the fulleroid vs methanofullerene isomers and, the more subtle, (ii) the valence tautomerization as a function of $d_{1,6}$ (open vs closed structure).

Regarding these issues, Prato et al.²⁹ suggested that the initial product of addition is a mixture of **11** and **14** on the basis of spectroscopic techniques and MNDO calculations and that the lowest energy isomer of substituted phenyldiazomethane and substituted diphenyldiazomethane addition has the structure **11**. After all, it has been a general consensus^{29,30} that the addition of carbene to C_{60} often generates [5,6] open fulleroid (**14**), as the kinetically controlled product, while the thermodynamically controlled product is the [6,6] closed methanofullerene, **11**. Osterodt and Vögtle³¹ have recently synthesized dibromomethanofullerene and suggested the [6,6] closed structure, **11a**, although their PM3 calculation yielded the [5,6] open structure, **14a**, as the most stable conformer by 4 kcal/mol. Li and Shevlin³² proposed another mechanism for the conversion of **14** to **11** on the basis of the triplet biradical intermediate, **13**.

According to simple electron counting, **12** should have 60 π -electrons as compared to 58 π -electrons of **11**. Furthermore, because of the sp^3 character of the bridgehead carbons in **11**, the four adjoining C–C bonds lost their partial π -bond character. Therefore, the 58 π -electrons are distributed over 58 carbons and 85 bonds in **11**, while, in the case of structure **12**, 60 π -electrons are distributed over 60 carbons and 89 bonds. Similarly 58 π -electrons are distributed over 85 bonds in **13** and 60 π -electrons are distributed in 89 bonds in **14**. Simple Hückel calculations yielded a rather large delocalization energy of 3.219β for **12** as compared to **11**. Structure **14** has a larger delocalization energy, 4.006β as compared to **13**. Interestingly, these extra stabilization energies are comparable to the value calculated for 1,6-methano[10]annulene (4β), as mentioned earlier. These simple calculations indicate that the aromatic stabilization of a fullerene in these ring opening reactions might be comparable to that of 1,6-methano[10]annulenes, raising the possibility of open structures (**12** and **14**) in fullerene and fulleroid derivatives.

TABLE 4: Calculated Geometries and Relative Energies of Methanofullerenes and Fulleroids^a

R	fulleroid [5,6] (13/14)				methanofullerene [6,6] (11/12)				E_{rel}^b
	$d_{1,2}$	$d_{1,6}$	$d_{1,61}$	Θ	$d_{1,2}$	$d_{1,6}$	$d_{1,61}$	Θ^c	
CH ₂	1.46	2.21	1.50	127	1.49	1.64	1.51	130 (152)	-0.1
CBr ₂	1.46	2.22	1.49	126	1.49	1.63	1.51	130 (140)	1.1
CF ₂	1.45	2.02	1.47	128	1.44	2.08	1.46	126 (146)	4.7
CO	1.46	2.20	1.47	127	1.49	1.72	1.48	129 (155)	-2.9

^a Geometric parameters are defined in **11** and **14**; bond lengths are in angstroms, by B3LYP/3-21G. ^b Energy difference between fulleroid and methanofullerene, in kilocalories per mole. ^c Bookfolding angle Θ is the angle between adjacent rings separated by $d_{1,6}$. In parentheses is the corresponding calculated value of the respective open methano[10]annulene, in degrees.

Full geometry optimizations on both [5,6]- and [6,6]-additions of simple fulleroids and methanofullerenes were performed with the B3LYP/3-21G method. The key parameters of these large-scale calculations are presented in Table 4. We will discuss three issues in the following order: structures of fulleroids, structures of methanofullerenes, and their relative energies.

Our full geometry optimizations—in agreement with expectations³⁰—show that all [5,6] fulleroids independently from the substituents have an open structure, **14**. The variations of the geometrical parameters around the substitution site are small, indicating that this structure is a stable and common feature of fulleroids. These structural results somewhat contradict the mechanism by Li and Shevlin,³² since one of the assumptions they made was the existence of the [5,6] closed form, **13**, making the biradical intermediate possible. The closed [5,6] form is a local minimum at the PM3 semiempirical level, but not in our DFT calculations.

The [6,6] substituted fullerene derivatives show a large variation as a function of substituents. The CH₂ and CBr₂ derivatives show closed structures (**11a** and **11b**) as the only minimum in the geometry optimization regardless of whether the optimization started from a closed or open structure. The CF₂ optimized structure is an open one (**12c**), while the CO shows an intermediate structure with an extremely elongated single bond (**11d**?).

The difference between CF₂ and CBr₂ is fully in line with our fragmentation model and steric hindrance arguments as well as with the trends found for the methano[10]annulenes. If the analogy with the methano[10]annulenes would be complete, we would expect an open structure for both CH₂ and CO methanofullerenes (**12a**, **12d**). The fact that the structure of the optimized CH₂ derivative is closed indicates that there is a substantial difference between the two groups of compounds regarding aromatic stabilization and steric constraints. The latter is indicated by the bookfolding angle, Θ . As can be seen from Table 4, the variations of the bookfolding angle are quite different in methanofullerenes from those in methano[10]annulenes, and their small variation indicates that the fullerene network resists the structural changes required by the substituted [10]annulene moiety. In the case of the CH₂ substitution the large reduction of the bookfolding angle from the [10]annulene value of 152° to 130° forces the bridgehead atoms to participate less in π -conjugation making their direct σ -bonding favorable. In the CBr₂ case the [10]annulene has a flat minimum, and it is therefore understandable why a smaller reduction of the bookfolding angle is sufficient to make the closed form more stable. In the CF₂ case the balance still seems to prefer an open structure. The discrepancy between the fullerene bookfolding angle and that of the methano[10]annulene is the largest in the CO case. It appears that the optimized $d_{1,6}$ value in this case is a compromise of the constraint on the bookfolding and the preference for an open structure yielding a somewhat peculiar bond length of 1.72 Å. It appears that there are substantial

differences between the valence tautomerization of methanofullerenes and methano[10]annulenes. Nevertheless, our calculations indicate that open [6,6] fullerene structures are possible, and we expect that their existence will be experimentally confirmed.

The calculated energy differences between the [5,6] and [6,6] structures are quite small, and the substituents can change the sign of the difference. The observed species is more dependent on the reaction mechanism than on their relative energetics.

Conclusions

On the basis of large-scale potential energy surface scans along the $d_{1,6}$ distance of 1,6-methano[10]annulene and its derivatives, the substituent effects on $d_{1,6}$ have been studied in the pursuit of understanding the X-ray crystallographic and temperature-dependent NMR results concerning the peculiarly long C—C bond values and their large variations as a function of substituents. The substituents mainly affect the relative stabilities between the bisnorcaradine form and the aromatic form, while the positions of the local minima along the variations of the bridgehead distance, $d_{1,6}$, are quite constant. According to the DFT calculations including electron correlation the potential energy surface has a low energy barrier between the two possible structures in agreement with the Woodward–Hoffmann rules.²⁶ The experimental data should be interpreted therefore in light of Simonetta's "fluxional" bonding that implies a small barrier resulting possibly in a large amplitude mode along the $d_{1,6}$ bond distance. These calculations are consistent with the experiment in terms of substitution trends. However, due to the slight overestimation of π -delocalization in the aromatic form, the exact details of the potential surface remain unresolved for the borderline cases of dimethyl, dibromo, and dicyano substituents.

The order in which the localized bisnorcaradine form (**1**) is favored over the delocalized aromatic form (**2**) is primarily determined by the energy difference of the singlet ground state of the respective substituted cyclopropane and the triplet ground state of corresponding substituted trimethylene. The dibromo substituted case shows that steric effects may tip the balance if the substituent is bulky. It seems that electronegativity of the substituents does not correlate well with the structural preferences of this valence tautomerism. Therefore, the 1/2 valence tautomerism of these molecules is the result of a low-lying trimethylene triplet state and its stabilization by aromatic delocalization over the two butadiene moieties.

The application of this picture yields predictions for the structural differences for disubstituted [5,6] and [6,6] ring junction adducts of C₆₀. All [5,6] disubstituted fulleroids studied here are predicted to have open structures in agreement with general expectations. However, in analogy to the methano[10]annulenes a substituent dependent variation of open and closed structures is calculated for [6,6] methanofullerenes, a prediction that awaits experimental tests.

Acknowledgment. We thank the National Science Foundation (Grant CHE-9601976) for financial support and the National Center for Supercomputing Applications (NCSA, Grant No. DMR-970017N) for the use of supercomputing facilities.

References and Notes

- (1) (a) Vogel, E.; Roth, H. D. *Angew. Chem., Int. Ed. Engl.* **1964**, *76*, 145. (b) Bianchi, R.; Pilati, T.; Simonetta, M. *J. Am. Chem. Soc.* **1981**, *103*, 6426. (c) Vogel, E.; Scholl, T.; Lex, J.; Hohlneicher, G. *Angew. Chem., Int. Ed. Engl.* **1982**, *21*, 869. (d) Gatti, C.; Barzaghi, M.; Simonetta, M. *J. Am. Chem. Soc.* **1985**, *107*, 878. (e) Domenicano, A., Hargittai, I., Eds. *Accurate Molecular Structures*; Oxford University Press: New York, 1992.
- (2) (a) Bianchi, R.; Morosi, G.; Mugnoli, A.; Simonetta, M. *Acta Crystallogr. B* **1973**, *29*, 1196. (b) Pilati, T.; Simonetta, M. *Acta Crystallogr. B* **1976**, *32*, 1912. (c) Bianchi, R.; Pilati, T.; Simonetta, M. *Acta Crystallogr. B* **1980**, *36*, 3146. (d) Bianchi, R.; Pilati, T.; Simonetta, M. *Acta Crystallogr. C* **1983**, *39*, 378. (e) Simonetta, M.; Barzaghi, M.; Gatti, C. *J. Mol. Struct.* **1986**, *138*, 39.
- (3) Stephens, P. W.; Bortel, G.; Faigel, G.; Tegze, M.; Jánossy, A.; Pekker, S.; Oszlanyi, G.; Forró, L. *Nature* **1994**, *370*, 636.
- (4) Choi, C. H.; Kertesz, M. *Chem. Phys. Lett.* **1998**, *282*, 318.
- (5) (a) Burgi, H. B.; Bartell, L. S. *J. Am. Chem. Soc.* **1972**, *94*, 5236. (b) Hagler, A. T.; Sharon, R.; Hwang, M.-J. *J. Am. Chem. Soc.* **1996**, *118*, 3759.
- (6) Toda, F.; Tanaka, K.; Stein, Z.; Goldberg, I. *Acta Crystallogr. C* **1996**, *52*, 177.
- (7) Choi, C. H.; Kertesz, M. *J. Chem. Soc., Chem. Comm.* **1997**, 2199.
- (8) Burgi, H. B.; Shefer, E.; Dunitz, J. D. *Tetrahedron* **1975**, *31*, 3089.
- (9) (a) Hoffmann, R. *Tetrahedron Lett.* **1970**, 2907. (b) Skanke, A.; Boggs, J. E. *J. Mol. Struct.* **1977**, *40*, 263. (c) Durmaz, S.; Kolmar, H. *J. Am. Chem. Soc.* **1980**, *102*, 6942.
- (10) Kaupp, G.; Boy, J. *Angew. Chem., Int. Ed. Engl.* **1997**, *36*, 48.
- (11) (a) Gunther, H.; Schmickler, H.; Bremser, W.; Straube, F. A.; Vogel, E. *Angew. Chem., Int. Ed. Engl.* **1973**, *12*, 570. (b) Arnz, R.; Carneiro, J. W.; Klug, W.; Schmickler, H.; Vogel, E.; Breuckmann, R.; Klärner, F. G. *Angew. Chem., Int. Ed. Engl.* **1991**, *30*, 683.
- (12) Frydman, L.; Frydman, B.; Kustanovich, I.; Vega, S.; Vogel, E.; Yannoni, C. S. *J. Am. Chem. Soc.* **1990**, *112*, 6472.
- (13) Dorn, H. C.; Yannoni, C. S.; Limbach, H.; Vogel, E. *J. Phys. Chem.* **1994**, *98*, 11628.
- (14) Klingensmith, K. A.; Püttmann, W.; Vogel, E.; Michl, J. *J. Am. Chem. Soc.* **1983**, *105*, 3375.
- (15) Bader, R. F. W. *Atoms in Molecules-A Quantum Theory*; Oxford University Press: Oxford, U.K., 1990.
- (16) Mealli, C.; Ienco, A.; Hoyt, E. B., Jr.; Zoellner, R. W. *Chem. Eur. J.* **1997**, *3*, 958.
- (17) Frisch, M. J.; Trucks, G. W.; Schlegel, H. B.; Gill, P. M. W.; Johnson, B. G.; Robb, M. A.; Cheeseman, J. R.; Keith, T.; Petersson, G. A.; Montgomery, J. A.; Raghavachari, K.; Al-Laham, M. A.; Zakrzewski, V. G.; Ortiz, J. V.; Foresman, J. B.; Cioslowski, J.; Stefanov, B. B.; Nanayakkara, A.; Challacombe, M.; Peng, C. Y.; Ayala, P. Y.; Chen, W.; Wong, M. W.; Andres, J. L.; Replogle, E. S.; Gomperts, R.; Martin, R. L.; Fox, D. J.; Binkley, J. S.; Defrees, D. J.; Baker, J.; Stewart, J. P.; Head-Gordon, M.; Gonzalez, C.; Pople, J. A. *Gaussian 94*, Revision E.1; Gaussian, Inc.: Pittsburgh, PA, 1995.
- (18) Lee, C.; Yang, W.; Parr, R. G. *Phys. Rev.* **1988**, *B37*, 785.
- (19) Becke, A. D. *J. Chem. Phys.* **1993**, *98*, 1372.
- (20) (a) Schleyer, P. v. R.; Maerker, C.; Dransfeld, A.; Jiao, H.; Eikema Hommes, N. J. R. v. *J. Am. Chem. Soc.* **1996**, *118*, 6317. (b) Jiao, H.; Schleyer, P. v. R. *Angew. Chem., Int. Ed. Engl.* **1996**, *35*, 2383. (c) Subramanian, G.; Schleyer, P. v. R.; Jiao, H. *Angew. Chem., Int. Ed. Engl.* **1996**, *35*, 2638.
- (21) (a) London, F. *J. Phys. Radium* **1937**, *8*, 397. (b) McWeeny, R. *Phys. Rev.* **1962**, *126*, 1028. (c) Dodds, J. L.; McWeeny, R.; Sadlej, A. J. *Mol. Phys.* **1980**, *41*, 1419. (d) Wolinski, K.; Hinton, J. F.; Pulay, P. *J. Am. Chem. Soc.* **1990**, *112*, 8251.
- (22) (a) Haddon, R. C.; Raghavachari, K. *J. Am. Chem. Soc.* **1985**, *107*, 289. (b) Almlöf, J.; Fisher, T. H.; Gassman, P. G.; Ghosh, A.; Haser, M. *J. Phys. Chem.* **1993**, *97*, 10964. (c) Choi, C. H.; Kertesz, M.; Karpfen, A. *J. Am. Chem. Soc.* **1997**, *119*, 11994.
- (23) Stevenson, G. R.; Zigler, S. S. *J. Phys. Chem.* **1983**, *87*, 895.
- (24) (a) Hoffmann, R. *J. Am. Chem. Soc.* **1968**, *90*, 1475. (b) Hoffmann, R.; Davidson, R. B. *J. Am. Chem. Soc.* **1971**, *93*, 5699. (c) Getty, S. J.; Hrovat, D. A.; Borden, W. T. *J. Am. Chem. Soc.* **1994**, *116*, 1521. (d) Baldwin, J. E.; Freedman, T. B.; Yamaguchi, Y.; Schaefer, H. F., III. *J. Am. Chem. Soc.* **1996**, *118*, 10934. (e) Greenberg, A.; Stevenson, T. A. In *Molecular Structure and Energetics*; Liebman, J. F., Greenberg, A., Eds.; VCH: Cambridge, U.K., 1986; Vol. 3.
- (25) Salem, L. *The Molecular Orbital Theory of Conjugated Systems*; W. A. Benjamin, Inc.: New York, 1966.
- (26) Woodward, R. B.; Hoffmann, R. *J. Am. Chem. Soc.* **1965**, *87*, 395.
- (27) For recent DFT analysis of pericyclic reactions, see: Wiest, O.; Houk, K. N. *Topics in Current Chemistry, Density Functional Theory IV*; Springer Verlag: New York, 1996.
- (28) (a) Suzuki, T.; Li, Q.; Khemani, K. C.; Wudl, F.; Almarsson, O. *Science* **1991**, *254*, 1186. (b) Wudl, F. *Acc. Chem. Res.* **1992**, *25*, 157. (c) For a recent review, see: Prato, M. *J. Mater. Chem.* **1997**, *7* (7), 1097.
- (29) Prato, M.; Lucchini, V.; Maggini, M.; Stimpfl, E.; Scorrano, G.; Eiermann, M.; Suzuki, T.; Wudl, F. *J. Am. Chem. Soc.* **1993**, *115*, 8479.
- (30) (a) Diederich, F.; Isaacs, L.; Philp, D. *J. Chem. Soc. Rev.* **1994**, 243. (b) Diederich, F.; Thilgen, C. *Science* **1996**, *271*, 317.
- (31) Osterodt, J.; Vögtle, F. *J. Chem. Soc., Chem. Comm.* **1996**, 547.
- (32) Li, Z.; Shevlin, P. B. *J. Am. Chem. Soc.* **1997**, *119*, 1149.